

Supplementary information

Exploration of $\text{Na}_7\text{Fe}_{4.5}(\text{P}_2\text{O}_7)_4$ as a cathode material for sodium-ion batteries

Yubin Niu,^{a,b} Maowen Xu,^{a,b,*} Bolei Shen,^{a,b} Chunlong Dai,^{a,b} and Chang Ming Li^{a,b,c,*}

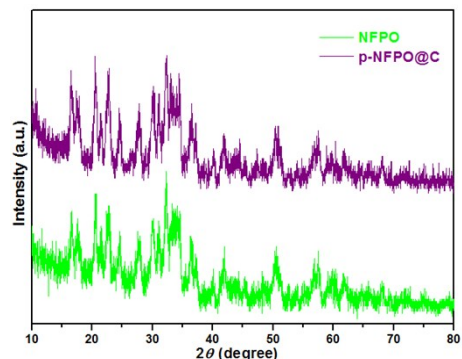


Fig. S1 XRD patterns of NFPO and p-NFPO@C, respectively.

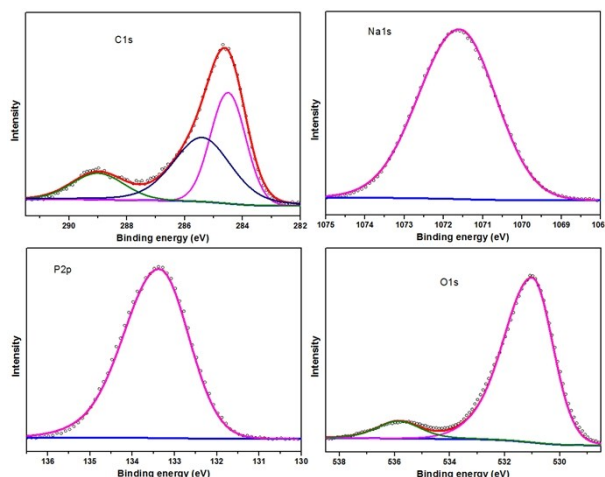


Fig. S2 XPS narrow spectra of the C 1s, Na 1s, P 2p and O 1s in p-NFPO@C composite, respectively.

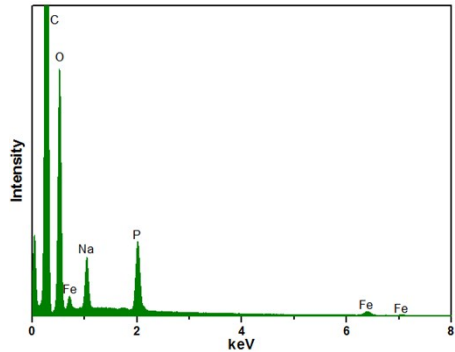


Fig. S3 The corresponding element composition diagram of p-NFPO@C.

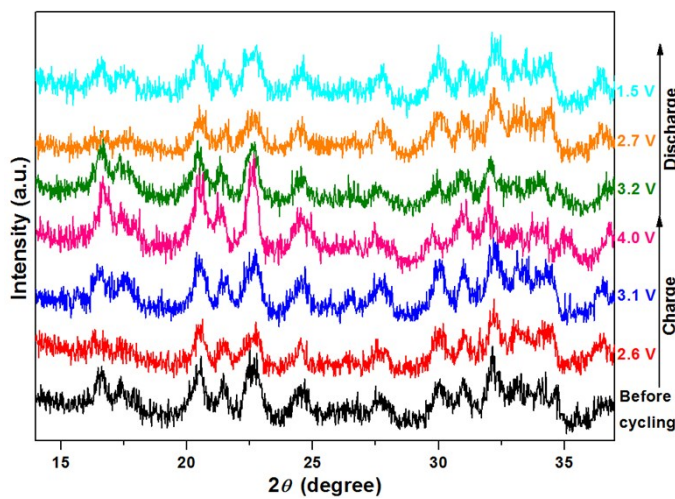


Fig. S4 Ex-situ XRD patterns of p-NFPO@C electrode at different states of charge and discharge, respectively.

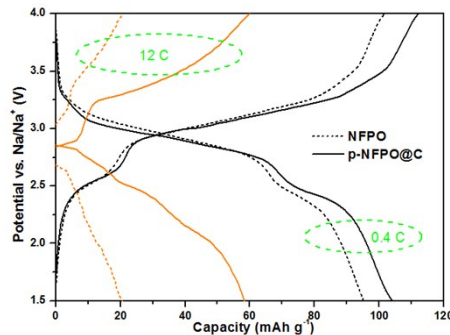


Fig. S5 Charge and discharge curves at 0.4 and 12 C of NFPO and p-NFPO@C, respectively.

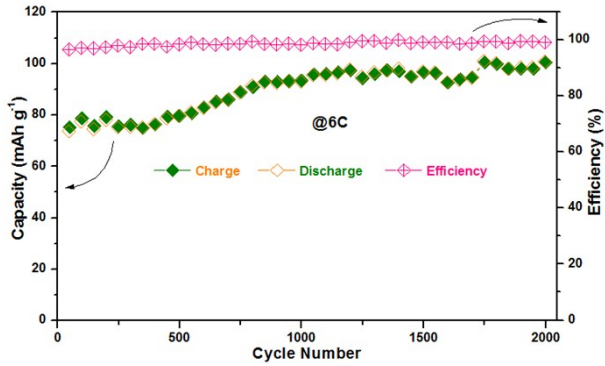


Fig. S6 Cycling performance and Coulombic efficiency of Na/p-NFPO@C cells at 6 C (648 mA g⁻¹).

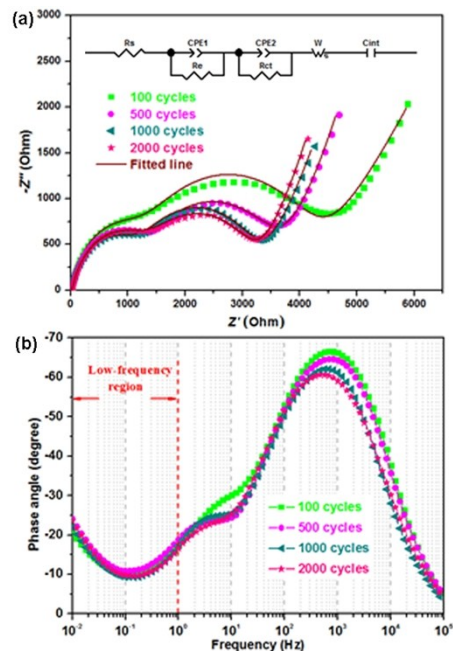


Fig. S7 Nyquist (a) and the corresponding Bode plots (b) of different cycles at 6 C in Na/p-NFPO@C cells. (Inset shows the equivalent circuit corresponding to the Nyquist plots.)

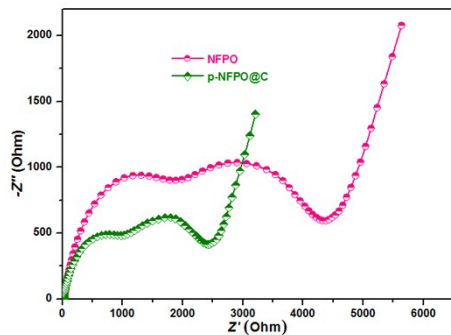


Fig. S8 EIS analysis of NFPO and p-NFPO@C at 6 C after 2000 cycles.

Table S1. Impedance parameters calculated from equivalent circuit.

Cycle	R _s (Ohm)	R _e (Ohm)	R _{ct} (Ohm)
100 th	12.3	839.8	2221
500 th	12.6	945.3	1603
1000 th	17.45	846.7	1481
2000 th	16.62	1006	1258